Preprints of the 21st IFAC World Congress (Virtual)
Berlin, Germany, July 12-17, 2020

Linear Time-Varying Model Predictive Control for Automated Vehicles: Feasibility and Stability under Emergency Lane Change ⋆

Yuchao Li * **Xiao Chen** * **Jonas Mårtensson** *

* *Division of Decision and Control Systems, School of Electrical Engineering and Computer Science, KTH Royal Institute of Technology, Stockholm, Sweden.* {yuchao, xiao2, jonas1}@kth.se.

Abstract: In this work, we present a novel approach based on linear matrix inequalities to design a linear-time varying model predictive controller for a nonlinear system with guaranteed stability. The proposed method utilizes a multi-model description to model the nonlinear system where the dynamics is represented by a group of linear-time invariant plants, which makes the resulting optimization problem easy to solve in real-time. In addition, we apply the control invariant set designed as the final stage constraint to bound the additive disturbance introduced to the plant by other subsystems interfacing with the controller. We show that the persistent feasibility is ensured with the presence of such constraint on the disturbance of the specified kind. The proposed method is then put into the context of emergency lane change for steering control of automated vehicles and its performance is verified via numerical evaluation.

Keywords: Model predictive control, stability, feasibility, automated vehicles.

1. INTRODUCTION

The past few decades has witnessed great advances in enabling technologies of automated vehicles. By removing human factors in driving, automated vehicles are widely expected to profoundly reshape our society and daily life. While many successful results have been reported, it is still too early to take the safety aspect for granted, especially under the shadow of a recent incident Knight (2018).

Among a chain of complex modules of an automated vehicle, the control unit for path tracking is one key component which plays a pivotal role in ensuring the safety. Although it is reasonable to assume it operates under nominal conditions at large, its capability to handle emergency shall never be overlooked. When something unexpected happens ahead, emergency lane change (ELC) is a common maneuver other than breaking. In fact, one study suggests that in many of those cases, the optimal maneuver would be steering alone (Llorca et al. (2011)). As a result, different aspects of ELC with different control techniques have been studied, Shiller and Sundar (1998); Swaroop and Yoon (1999); Llorca et al. (2011); Vanholme et al. (2013), to name a few.

In recent years, model predictive control (MPC) has been recognized as another promising approach for vehicle control and has gained significant attention. Although in theory, two essential aspects of MPC, namely feasibility of obtaining a numerical solution and stability of the resulting closed-loop system, have been well studied (refer to Mayne et al. (2000) and references therein), the formal analysis of them can be found absent in practice due to implementation difficulties (Falcone et al. (2007)). In those cases, extensive tests are carried out to verify the control functionality, but it may as well be inadequate in scenarios like ELC. To address the problem, an additional convex constraint is introduced by Falcone et al. (2008) to ensure stability. However, the resulting MPC is cast as a Sequential Quadratic Program (SQP), which is relatively burdensome compared to Quadratic Program (QP). Inspired by the multi-plant description in Kothare et al. (1996), where a linear-time varying (LTV) system is described by a class of linear time-invariant (LTI) models, Lima et al. (2017a) propose a MPC controller which allows the resulting MPC to be solved as a QP problem with guaranteed stability, and the method exhibits its capacity in field experiments (Lima et al. (2018a)). However, the lattice-based design procedure for the final stage cost introduced in those works requires analytical ingenuity and the output of the procedure fulfills a necessary, not sufficient condition for stability, which means the designed final stage cost needs to go through all LTI model description to verify its correctness after one design iteration, which results in an iterative procedure for computing the final stage cost alone.

In addition, the ELC scenarios may impose a new challenge on the feasibility problem. In the methods introduced above, the persistent feasibility of obtaining a solution is guaranteed by proper design of final stage constraint once it's initially feasible, which is known as recursive feasibility. However, such a property is obtained with the assumption that the initialization procedure would not repeat while operating. When an abrupt change of lanes occurs, it may be regarded as another initiation should the provided reference not be executable, which is significantly different from the one occurred during ignition. By executable, here we mean the reference is physically feasible to follow or at least leads to a numerically feasible solution of the controller. Although it is reasonable to assume the reference path provided by the planning unit is executable for the controller, such an assumption would indeed be more

⋆ This work was supported by the Swedish Research Council,and the Swedish Foundation for Strategic Research.

plausible if a certain metric is provided by the controller itself to indicate the numerical feasibility of the provided reference candidate. Similar discussion, although not within the context of ELC, is found in Simon et al. (2012).

This paper extends our previous works (Lima et al. (2017a, 2018a)) and the approach presented here features the following new contributions:

(1) the computation of the final stage cost, which is used to ensure the closed-loop stability, is cast as linear matrix inequalities (LMIs) to greatly ease the design procedure;
(2) the feasibility of LTV-MPC under a change of set points are analyzed and a bound is introduced as a sufficient condition to ensure the feasibility of those changes;
(3) the vehicle control problem in the ELC scenario is put in connection with the feasibility and stability analysis of LTV-MPC under set point changes and its performance is examined via numerical evaluation.

The rest of this paper is organized as follows. Section 2 presents the preliminaries of LTV-MPC and notations applied here. Section 3 reminds the computation of final stage constraints and final stage cost without disturbance via multi-model representation. Sections 4 introduces the bound for the disturbance to ensure feasibility and a LMI formulation for the design of the final stage cost, and the proposed method is tested via numerical evaluation in an emergency lane change scenario in Section 5. Section 6 concludes the paper.

2. PRELIMINARIES ON LTV-MPC

In this section, we introduce the preliminaries on LTV-MPC. We deal with discrete-time nonlinear systems subject to external inputs and additive disturbance on the states:

$$z(k+1) = f(z(k), u(k)) + \omega(k) \tag{1}$$

where $z(k) \in \mathbb{R}^n$ and $u(k) \in \mathbb{R}^m$ are state and input vectors respectively. $\omega(k) \in \mathbb{R}^n$ are undesired change introduced by other subsystems interfacing with the control unit and therefore regarded as disturbance by the controller. The system is subject to state and input constraints

$$z(k) \in \mathcal{Z},\ u(k) \in \mathcal{U},\ \Delta u(k) \in \Delta\mathcal{U},\ \forall k \in \mathbb{N}_+ \tag{2}$$

where the sets $\mathcal{Z} \subseteq \mathbb{R}^n$ and $\mathcal{U}$, $\Delta\mathcal{U} \subseteq \mathbb{R}^m$ are polytopes, and $\Delta u(k) = u(k) - u(k-1)$. Regarding $\omega(k)$, we make the following assumption:

Assumption 2.1. $\omega(k) \neq 0$ only if $z(k)$ is within certain polytope $\mathcal{Z}_w \subseteq \mathcal{Z}$.

Such an assumption is plausible since $\omega(k)$ is used to model undesired change from other subsystems. Within the context of ELC, this disturbance comes from the path planning module of the vehicle. Within our scope, the disturbance shall be checked to fulfill the constraint

$$\omega(k) \in \mathcal{W} \subseteq \mathcal{Z},\ \forall k \in \mathbb{N}_+ \tag{3}$$

where $\mathcal{W}$ is to be designed, as is $\mathcal{Z}_w$.

Now consider the problem of controlling the discrete-time nonlinear system (1) with constraints (2) to track a given time-varying reference when $z(k) \in \mathcal{Z} \setminus \mathcal{Z}_w$. Under Assumption 2.1, $\omega(k)$ is absent. Denote the reference states and inputs as $z_r(k) \in \mathcal{Z}$ and $u_r(k) \in \mathcal{U}$ and assume it is a solution of Eq. (1) when $\omega(k) = 0$. Let $\bar{Z}_r(k) = \{z_r(k),\ z_r(k+1),\ ...\}$ be the reference state path obtained by applying an input sequence $\bar{U}_r(k) = \{u_r(k),\ u_r(k+1),\ ...\}$. Then by first order Taylor expension, we obtain

$$\tilde{z}(k+1) = A(\xi(k))\tilde{z}(k) + B(\xi(k))\tilde{u}(k) \tag{4}$$

where $\tilde{z}(k) = z(k) - z_r(k)$ and $\tilde{u}(k) = u(k) - u_r(k)$ and

$$A(\xi(k)) = \frac{\partial f(z,\,u)}{\partial z}\Big|_{\substack{z=z_r\\u=u_r}},\ B(\xi(k)) = \frac{\partial f(z,\,u)}{\partial u}\Big|_{\substack{z=z_r\\u=u_r}} \tag{5}$$

where $\xi(k)$ is a parameter vector of the form $\xi(k) = [z_r(k)^T\ u_r(k)^T]^T$, which is known at each step k. Besides, $\xi(k) \in \Xi$ where Ξ is a closed set given by

$$\Xi = \{\xi \in \mathbb{R}^{m+n} : \xi_{\min} \leq \xi \leq \xi_{\max}\} \tag{6}$$

where the inequality operations are considered element-wise.

Let $\gamma \in \Gamma$ represent a model described by a specific pair $(A(\xi), B(\xi))$, where the set Γ is a multi-plant description defined as

$$\begin{aligned}\Gamma = \{(A, B) \in \mathbb{R}^{m\times m} \times \mathbb{R}^{m\times n} :\\ A = A(\xi), B = B(\xi), \xi \in \Xi\}.\end{aligned} \tag{7}$$

Note that each $\gamma \in \Gamma$ is time-invariant and depends on a (known) parameter ξ. In addition, we assume $|\Gamma| < \infty$.

Assume that a full measurement or estimate of the state $z(t)$ is available at the current time t. Then, the following MPC problem can be formulated

$$\min_{\tilde{U}_t} \quad \tilde{z}_{t+N|t}^T Q_f \tilde{z}_{t+N|t} + \sum_{k=t}^{t+N-1} \tilde{z}_{k|t}^T Q \tilde{z}_{k|t} + \tilde{u}_{k|t}^T R \tilde{u}_{k|t} \tag{8a}$$

$$\text{s. t.} \quad \tilde{z}_{k+1|t} = A\big(\xi(k|t)\big)\tilde{z}_{k|t} + B\big(\xi(k|t)\big)\tilde{u}_{k|t},\ k = t, ..., t+N-1, \tag{8b}$$

$$\Delta u_{k+1|t} = u_{k+1|t} - u_{k|t},\ k = t, ..., t+N-1, \tag{8c}$$

$$\tilde{z}_{k|t} \in \tilde{\mathcal{Z}},\ k = t, ..., t+N-1, \tag{8d}$$

$$u_{k|t} \in \mathcal{U},\ k = t, ..., t+N-1, \tag{8e}$$

$$\Delta u_{k|t} \in \Delta\mathcal{U},\ k = t, ..., t+N-1, \tag{8f}$$

$$\tilde{z}_{t+N|t} \in \tilde{\mathcal{Z}}_f, \tag{8g}$$

$$\tilde{z}_{t|t} = \tilde{z}(t), \tag{8h}$$

$$\Delta u_{t|t} = u(t) - u(t-1), \tag{8i}$$

where $\tilde{U}_t = \{\tilde{u}_{t|t}, ..., \tilde{u}_{t+N-1|t}\}$ is the sequence of inputs to be optimized, which are constrained to be in a convex polytope $\mathcal{U}$. The difference between the state vector at time $t+\ell$ predicted at time t and the reference state vector $z_r(t+\ell)$ is defined as $\tilde{z}_{t+\ell|t}$ where $\ell = 0, 1, ..., N$. The difference between the predicted and the reference state is constrained to be in a convex polytope $\tilde{\mathcal{Z}}$. The predicted difference of inputs between $t+\ell+1$ and $t+\ell$, denoted as $\Delta u_{t+\ell+1|t}$, is constrained to be in a convex polytope $\Delta\mathcal{U}$. Here, the notation $z_{t+\ell|t}$ stands for the state z at time $t+\ell$ predicted at time t. The notation is analogous for $u_{t+\ell|t}$ and $\Delta u_{t+\ell|t}$. Note that $z(t)$ is then the actual state z at time t, and $u(t)$ and $u(t-1)$ are actual inputs at t and $t-1$ respectively. The matrices R, Q, and Q_f are positive definite and penalize deviations from the reference input, state, and terminal state, respectively.

In addition, we introduce some concepts from Borrelli et al. (2017) to address the feasibility problem. The following definitions are with regards to the system (1) with constraint (2) under Assumption 2.1 and $z(k) \in \mathcal{Z} \setminus \mathcal{Z}_w$.

Definition 2.1. We denote the one-step controllable set with regard to some target set $\mathcal{S} \subseteq \mathcal{Z}$ as

$$\mathrm{Pre}(\mathcal{S}) = \{z \in \mathbb{R}^n : \exists u \in \mathcal{U}, f(z, u) \in \mathcal{S}\}. \tag{9}$$

Definition 2.2. The N-step controllable set with regard to some target set $\mathcal{S} \subseteq \mathcal{Z}$ is defined recursively as

$$\mathcal{K}_j(\mathcal{S}) = \mathrm{Pre}(\mathcal{K}_j(\mathcal{S})) \cap \mathcal{Z},\ \mathcal{K}_0(\mathcal{S}) = \mathcal{S} \tag{10}$$

for $j = \{1, ..., N\}$.

Definition 2.3. A set $\mathcal{O} \subseteq \mathcal{Z}$ is said to be a positive invariant set if

$$z(0) \in \mathcal{O} \implies z(k) \in \mathcal{O},\ \forall k \in \mathbb{N}_+.$$

Definition 2.4. A set $\mathcal{O}_\infty \subseteq \mathcal{Z}$ is said to be the maximal positive invariant set if

$$\mathcal{O}_\infty = \cup_{i \in \mathcal{I}} \mathcal{O}_i$$

where $\mathcal{I}$ indexing the family of invariant sets.

In addition, given certain predefined feedback control law $l(k)$, the system would become autonomous one, namely

$$z(k+1) = f_a(z(k)) + \omega(k) \tag{11}$$

where $f_a(z(k)) = f(z(k), l(k)z(k))$. For such autonomous system, all above definitions can be defined analogously.

Theorem 2.5. (Theorem 10.1 in Borrelli et al. (2017)) A set $\mathcal{O} \subseteq \mathcal{Z}$ is a positive invariant set for autonomous system (11) under constraint (2) with $\omega(k) = 0$ if and only if

$$\mathcal{O} \subseteq \mathrm{Pre}(\mathcal{O}). \tag{12}$$

3. STABILITY AND FEASIBILITY WITHOUT DISTURBANCE

In this section, we recall the results derived in Lima et al. (2017a, 2018a) when $\omega(k)$ is absent. For LTI model, a typical choice for $\tilde{\mathcal{Z}}_f$ is the maximal positive invariant set $\mathcal{O}_\infty^{\mathrm{LQR}}$ for the closed-loop system

$$\tilde{z}(k+1) = \big(A(\xi) + B(\xi)L_{\mathrm{LQR}}(\xi)\big)\tilde{z}(k), \tag{13}$$

where $\xi \in \Xi$ here is a fixed vector and L_{LQR} is the associated LQR gain (i.e., the unconstrained infinite time optimal controller gain).

However, under multi-model description, there are several maximal positive invariant sets $\mathcal{O}_\infty^{\mathrm{LQR}}(\gamma)$ and several different LQR feedback controllers $L_{\mathrm{LQR}}(\xi)$, one for each $\xi \in \Xi$. Therefore, the maximal positive invariant set $\bar{\mathcal{O}}_\infty^{\mathrm{LQR}}$ for the LTV plant, by Theorem 2.5, shall fulfill $\bar{\mathcal{O}}_\infty^{\mathrm{LQR}} \subseteq \mathrm{Pre}_\gamma(\bar{\mathcal{O}}_\infty^{\mathrm{LQR}}),\ \forall \gamma \in \Gamma$ where $\mathrm{Pre}_\gamma(\cdot)$ is with respect to autonomous system under LQR control law for LTI model γ. With absence of disturbance $\omega(k)$, the following result is derived with regards to the system (1) under constraint (2) in Lima et al. (2018a) as

$$\bar{\mathcal{O}}_\infty^{\mathrm{LQR}} = \lim_{k \to \infty} \Omega_k \tag{14}$$

where Ω_k is computed recursively as

$$\Omega_{k+1} = \bigcap_{\gamma \in \Gamma} \mathrm{Pre}_\gamma(\Omega_k) \cap \Omega_k,\ \Omega_0 = \tilde{\mathcal{Z}}$$

Regarding closed-loop stability, when the model is LTI (i.e., for a specific $\xi \in \Xi$), the control law $u(t) = L_{\mathrm{LQR}}(\xi)\tilde{z}(t)$ would result in an infinite-horizon cost given by

$$J_\infty^*\big(\tilde{z}(t)\big) = \tilde{z}(t)^T P(\xi)\tilde{z}(t) = \sum_{k=t}^{\infty} \tilde{z}_{k|t}^T Q \tilde{z}_{k|t} + \tilde{u}_{k|t}^T R \tilde{u}_{k|t}, \tag{15}$$

where $P(\xi)$ is given by the solution of the algebraic Riccati equation for the system (4) for a specific $\xi \in \Xi$, i.e.,

$$A(\xi)^T \Big(P(\xi) - P(\xi)B(\xi)\big(B(\xi)^T P(\xi)B(\xi) + R\big)^{-1} B(\xi)P(\xi)\Big)A(\xi) + Q - P(\xi) = 0, \tag{16}$$

which can be rewritten as

$$A_{\mathrm{cl}}(\xi)^T P(\xi) A_{\mathrm{cl}}(\xi) + L_{\mathrm{LQR}}(\xi)^T R L_{\mathrm{LQR}}(\xi) + Q - P(\xi) = 0, \tag{17}$$

where $A_{\mathrm{cl}}(\xi) = \big(A(\xi) + B(\xi)L_{\mathrm{LQR}}(\xi)\big)$. Therefore, the terminal cost $\tilde{z}_{t+N|t}^T Q_f \tilde{z}_{t+N|t}$ is typically chosen as the solution of the algebraic Riccati equation for the system (4) for a given $\xi \in \Xi$.

To prove the closed-loop stability through Lyapunov techniques for LTV-MPC, a lattice based method is introduced in Lima et al. (2018a) where some candidate $\bar{P}$ that is positive definite is obtained and then verified to check if

$$A_{\mathrm{cl}}(\xi)^T \bar{P} A_{\mathrm{cl}}(\xi) + L_{\mathrm{LQR}}(\xi)^T R L_{\mathrm{LQR}}(\xi) + Q - \bar{P} \preceq 0, \tag{18}$$

holds $\forall \xi \in \Xi$. Via such iterative procedure, if $\bar{P}$ fulfills (18), then the closed loop stability is ensured. The following results are proven in Lima et al. (2018a). The narratives are slightly modified to fit the notion here and the system concerned is without disturbance $\omega(k)$.

Theorem 3.1. (Theorem 5.1 in Lima et al. (2018a)) The problem (8) is feasible for all $t \geq 0$ if $Q_f = \bar{P}$, $\tilde{\mathcal{Z}}_f = \bar{\mathcal{O}}_\infty^{\mathrm{LQR}}$, and if $\tilde{z}(0) \in \mathcal{K}_N(\bar{\mathcal{O}}_\infty^{\mathrm{LQR}})$.

Theorem 3.2. (Theorem 5.2 in Lima et al. (2018a)) Consider the model (1) under constraint (2) without disturbance $\omega(k)$, and the LTV-MPC controller (8). Assume there is no external disturbance. The terminal penalty matrix Q_f is chosen as $\bar{P}$, and the terminal constraint $\tilde{\mathcal{Z}}_f$ is chosen as $\bar{\mathcal{O}}_\infty^{\mathrm{LQR}}$. Then, the state of the closed-loop system converges to the origin. Moreover, the origin of the closed-loop system is asymptotically stable with domain of attraction $\mathcal{K}_N(\bar{\mathcal{O}}_\infty^{\mathrm{LQR}})$.

4. MAIN RESULTS

Under Assumption 2.1, when $\omega(k) \neq 0$, $\mathcal{W}$ is ought to be present for other subsystems, which introduce $\omega(k)$ to the controller, in order to ensure the feasibility of the control law, and indeed it can be computed based on the results in Theorem 3.1.

Theorem 4.1. Given $\mathcal{Z}_w$. Let Assumption 2.1 hold. The recursive feasibility is ensured if the disturbance constraint $\mathcal{W}$ fulfill

$$\mathcal{W} \oplus \mathcal{Z}_w = \bar{\mathcal{O}}_\infty^{\mathrm{LQR}}, \tag{19}$$

where $\oplus$ denote the Minkowski addition.

Proof. When $\omega(k) \neq 0$, the control problem (8) can be viewed to have a new initialization. By Theorem 3.1, under Assumption 2.1, since $\bar{\mathcal{O}}_\infty^{\mathrm{LQR}} \subseteq \mathcal{K}_N(\bar{\mathcal{O}}_\infty^{\mathrm{LQR}})$ the feasibility can be ensured if (19) holds.

Remark 4.1.1. According to Theorem 3.1, if the disturbance constraint fulfills

$$\mathcal{W} \oplus \mathcal{Z}_w = \mathcal{K}_N(\bar{\mathcal{O}}_\infty^{\mathrm{LQR}}),$$

the resulting system would have a feasible initial condition. However, it is intractable to explicitly compute $\mathcal{K}_N(\bar{\mathcal{O}}_\infty^{\mathrm{LQR}})$ since it is dependent on γ. On the other hand, it is not easy either to verify if $\tilde{z}+\omega \in \mathcal{K}_N(\bar{\mathcal{O}}_\infty^{\mathrm{LQR}})$ since both $\tilde{z}$ and ω are not available offline. Note that in Theorem 3.1 $\tilde{z}(0) \in \mathcal{K}_N(\bar{\mathcal{O}}_\infty^{\mathrm{LQR}})$ since $\tilde{z}(0)$ is the system state during true initialization, which is available offline.

Besides, the lattice based approach ensure a necessary condition is fulfilled, which as a result require verification of inequality (18) once a candidate $\bar{P}$ is obtained. Although the analytical solution for (23) may not be easy to obtain, the existence of such a $\bar{P}$ can be sought via Linear Matrix Inequalities (LMI) approach, as is given below.

Theorem 4.2. Consider the model (1) under constraint (2) and let Assumption 2.1 hold. The soughted $\bar{P}$ in Theorem 3.2 is any solution of the following LMIs:

$$\begin{bmatrix} \bar{P} & \bar{P}A_{\mathrm{cl}}(\xi) \\ A_{\mathrm{cl}}(\xi)^T\bar{P} & \bar{P}+\Delta V(\xi) \end{bmatrix} \succeq 0,\ \forall \xi \in \Xi, \tag{20}$$

where $\Delta V(\xi)$ is given as

$$\Delta V(\xi) = A_{\mathrm{cl}}(\xi)^T P(\xi) A_{\mathrm{cl}}(\xi) - P(\xi). \tag{21}$$

Proof. By Theorem 3.2, we are seeking positive-definite $\bar{P}$ such that (18) holds $\forall \xi \in \Xi$. However, by (17), we have

$$L_{\mathrm{LQR}}(\xi)^T R L_{\mathrm{LQR}}(\xi) + Q = P(\xi) - A_{\mathrm{cl}}(\xi)^T P(\xi) A_{\mathrm{cl}}(\xi). \tag{22}$$

Plugging (22) into (18), we have

$$A_{\mathrm{cl}}(\xi)^T\big(\bar{P} - P(\xi)\big)A_{\mathrm{cl}}(\xi) - \big(\bar{P} - P(\xi)\big) \preceq 0. \tag{23}$$

Note that (23) can be viewed as a Schur complement of block $\bar{P} + \Delta V(\xi)$ in (20). Therefore, LMIs in (20) is equivalent to ensure (23) to hold and $\bar{P}$ to be positive definite simultaneously. As a result, the LMI conditions here are sufficient and necessary for (18) to hold $\forall \xi \in \Xi$ and for the cost function (8a) to be a valid Lyapunov candidate. Given a $\bar{P}$ which fulfills (20), the cost function (8a) can then be applied as Lyapunov candidate for the stability analysis. It can be shown that the cost is nonincreasing due to (18). Details of this derivation can be found in Lima et al. (2018a).

5. AUTOMATED VEHICLE APPLICATION

In this section, we apply the LTV-MPC framework introduced above to an automated truck and test its performance via numerical evaluations. The test scenario is a road with two obstacles, 40 meters apart from each other, which is immediately followed by a steep curve, as is illustrated in Fig. 1. Within such a situation, the truck can become unstable easily, as is the case for the controller without the final state cost, while our proposed LTV-MPC controller manages to stabilize the truck while ensuring feasibility under multiple ELCs.

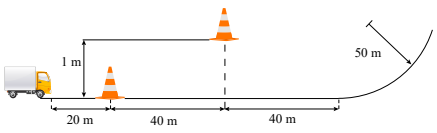

Fig. 1. The scenario for LTV-MPC controller stability test. For the purpose of clear presentation, the scale in the figure is not consistent.

5.1 Spatial vehicle model for controller design

We apply the spatial vehicle model introduced in Gao et al. (2012) for controller design. Via such a model, the deviation from path central line and correct heading can be directly addressed. In addition, the model can be applied to address other criteria, such as accuracy and smoothness of tracking, which is verified in the field tests in Lima et al. (2017b).

The nonlinear bicycle in the road aligned framework is shown in Fig. 2 and its dynamics is given as

$$\begin{aligned} e_y' &= \frac{\rho_s - e_y}{\rho_s}\tan(e_\psi), \\ e_\psi' &= \frac{(\rho_s - e_y)}{\rho_s\cos(e_\psi)}\kappa - \psi_s'. \end{aligned} \tag{24}$$

where s denotes the position align the road central line, e_y is the deviation from the central line, e_ψ is the heading error, ρ_s is the radius of curvature of the road and ψ_s is the road heading angle. The derivatives are taken with respect to s. The vehicle curvature κ is related with the vehicle steering angle δ by $\kappa = \frac{\tan(\delta)}{l}$ where l is the distance between front and rear wheels.

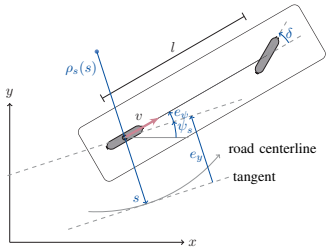

Fig. 2. A nonlinear bicycle model in the road aligned framework Lima et al. (2017a).

Via linearization and discretization around a reference path $z_r(k) = [e_{y,r}(k), e_{\psi,r}(k)]^T = [0,0]^T$ for all $k \geq 0$ given by a reference sequence of inputs $\bar{U}_r(k)$, if Δs is assumed to be constant, a LTV model of the form (4) when disturbance is absent can be obtained as follows

$$\begin{bmatrix} e_y(k+1) \\ e_\psi(k+1) \end{bmatrix} = \begin{bmatrix} 1 & \Delta_s \\ -\kappa_r^2(k)\Delta_s & 1 \end{bmatrix}\begin{bmatrix} e_y(k) \\ e_\psi(k) \end{bmatrix} + \begin{bmatrix} 0 \\ \Delta_s \end{bmatrix}\tilde{\kappa}(k), \tag{25}$$

where $\kappa_r = \kappa_s = \frac{1}{\rho_s}$ is the curvature of reference path.

5.2 Computation of the final state constraint

With system dynamics (24), the final stage constraint is computed by (14). Here we design the $\mathcal{Z}_w$ to be in the vicinity of the origin and $\mathcal{W}$ can be obtained accordingly. All the computations are carried out via MPT toolbox in MATLAB Herceg et al. (2013). One of such results for a perticular design of $\mathcal{Z}_w$ is shown in Fig. 3.

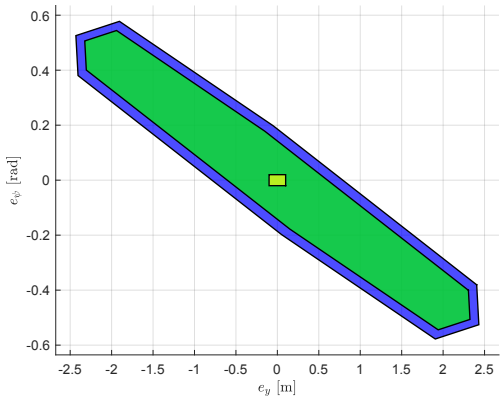

Fig. 3. Given the design of $\mathcal{Z}_w$, $\mathcal{W}$ is obtained via (19).

During an ELC, a higher-level path planner generates a lane change distance modelled as $w(t)$, which is compared to the disturbance set $\mathcal{W}$ to ensure the persistent feasibility of the controller. A visualization of their relations in an ELC scenario is shown in Fig. 4. In this case, the magnitude of ELC is within $\mathcal{W}$.

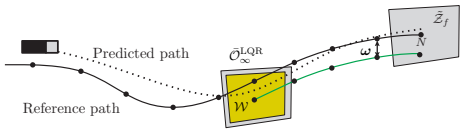

Fig. 4. An ELC is planned to occur at $k = 5$ where the changed lane is in green and the set $\mathcal{W}$ in yellow. In this particular illustration, such ELC would be regarded as feasible since $\tilde{z}(5) + \omega(5) \in \bar{\mathcal{O}}_\infty^{\mathrm{LQR}}$.

5.3 Computation of the final stage cost

As for the final stage cost $\bar{P}$ with model (25), we solve the LMIs (20) while minimizing the trace of $\bar{P}$. We plot out the ellipse of $x^T\big(\bar{P}-P(\xi)\big)x = 1$ in solid line and $x^T A_{\mathrm{cl}}(\xi)^T\big(\bar{P}-P(\xi)\big)A_{\mathrm{cl}}(\xi)x = 1$ in dashed line. The ellipses with the same γ are in the same color. $x^T\big(\bar{P} - P(\xi)\big)x = 1$ is always encircled by $x^T A_{\mathrm{cl}}(\xi)^T\big(\bar{P} - P(\xi)\big)A_{\mathrm{cl}}(\xi)x = 1$ for the same γ, which indicates (23) hold, and consequently the values of Lyapunov function is decreasing.

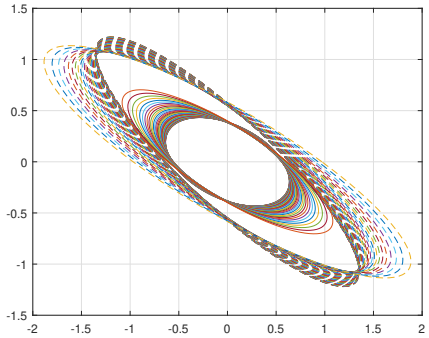

Fig. 5. The ellipses of of $x^T\big(\bar{P} - P(\xi)\big)x = 1$ and $x^T A_{\mathrm{cl}}(\xi)^T\big(\bar{P} - P(\xi)\big)A_{\mathrm{cl}}(\xi)x = 1$ with different ξ.

5.4 Dynamic vehicle model for verification

We apply the dynamic vehicle model with 2 wheel axles of trucks as the plant to test the performance of the proposed LTV-MPC. We choose trucks to evaluate the controller performance as they have less maneuverability as opposed to small vehicles, and they can operate in closed environments for industrial operations, which increases the chance of having fully-automated functions deployed in the near future, as opposed to those driving in the public traffic network.

The dynamic vehicle model is given by

$$\begin{aligned} m(\dot{v}_x - \dot{\psi}v_y) &= F_x - F_{y_f}\sin\delta, \\ m(\dot{v}_y + \dot{\psi}v_x) &= F_{y_b} + F_{y_f}\cos\delta, \\ J_z\ddot{\psi} &= fF_{y_f}\cos\delta - bF_{y_b}, \end{aligned}$$

where v_x and v_y are velocities in longitudinal and lateral directions in the vehicle frame respectively, and since our focus is lateral control, v_x holds constant in our simulation. $\dot{\psi}$ is the yaw rate, δ is the steering angle of front wheels. Model parameters m, J_z, f, b are constants. The side forces are linear functions of slip angles given by

$$F_{y_f} = -C_f\alpha_f,\ F_{y_b} = -C_b\alpha_b,$$

where C_b and C_f are stiffnesses of the rear and the front axles, respectively, and the slip angles are given

$$\alpha_f = \arctan\Big(\frac{v_y + \dot{\psi}f}{v_x}\Big) - \delta,\ \alpha_b = \arctan\Big(\frac{v_y - \dot{\psi}b}{v_x}\Big).$$

The relation between the curvature of the vehicle and its steering angle can be described by

$$\delta = \arctan\big((l + k_{us}v_x^2)\kappa\big),$$

where $l = b+f$ and k_{us} is the understeer gradient of the vehicle.

The model has been widely applied as it represents well the vehicle dynamics, and the set of model parameters we use here are from Lima et al. (2018b). The value of the understeer gradient is computed by its relation to m, b, f, l, C_f, and C_b given in Dixon (1996).

5.5 Numerical evaluation

For our numerical evaluation, we set the vehicle speed as 10 m/s and initially 20 m away from the first obstacle. We have the state cost matrix Q as a diagonal one with Q_{11} to be set in different values and Q_{22} fixed. The input cost parameter R is fixed. Since the purpose here is to test the feasibility and the stability of the controller, those parameters are not fine-tuned. The LTV-MPC controller runs 50 Hz on the vehicle while the discretization step for (25) in the controller design is 0.1 s. Such a setup is initially suggested by Gao et al. (2012) and has been proven to work well in the previous field tests reported by Lima et al. (2018a). The controller parameters are summarized in Table 1.

Table 1. Controller parameters (SI units)

Q_{22}	R	N	$e_y^{\max}$	$e_\psi^{\max}$	$\kappa^{\max}$	$\dot{\kappa}^{\max}$	l
10	10	9	4	0.8	0.18	0.05	4

The numerical results of states and inputs for Q_{11} being 2 and 3 are shown in Fig. 6 and Fig. 7 respectively. The first ELC is performed at $t = 0$ s while the second is at $t = 4$ s. In the case where both controllers lead to stable trajectories, the one with the final stage cost outperforms the one without the Q_f term, while in the other case when $Q_{11} = 3$, the controller with Q_f term leads to a slightly faster rise time of e_y (1.4 s, as opposed to 1.52 s when $Q_{11} = 2$), while the one without Q_f leads to an unstable closed-loop system. Notice that in the cases where the final stage cost in place, there are small offsets of e_y in both Figs. 6 and 7, with magnitudes of 0.09 and 0.08 m respectively. This is due to that (25) used for prediction in control neglects the lateral friction which is present in the simulation model. Compared with the size of the vehicle, such small offset is acceptable.

In addition, the lane change distance, modelled as $\omega(t)$ in our approach, is compared to the disturbance set $\mathcal{W}$ to ensure the persistent feasibility of the system.

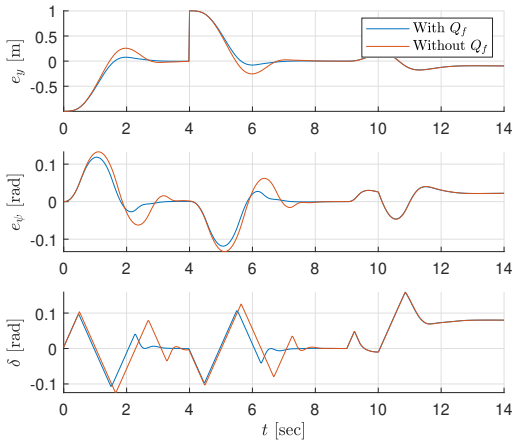

Fig. 6. States and control with and without final stage costs where $Q_{11} = 2$.

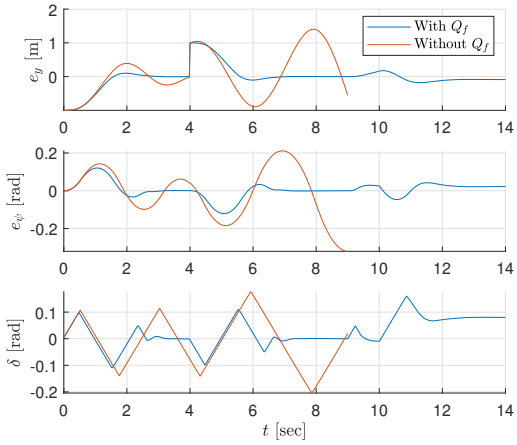

Fig. 7. States and control with and without final stage costs where $Q_{11} = 3$.

6. CONCLUSION

In this paper, a LMI based approach is presented for LTV-MPC design. The resulting control law has guaranteed stability for the closed-loop system and persistent feasibility of the optimization problem under certain additive disturbance from other interfacing system can be ensured via utilizing the final stage constraint, which is computed offline. The proposed method is applied for steering control for automated vehicle application in an ELC scenario and its capacity is justified through numerical evaluation.

As for future work, we would like to investigate the potentials of the control invariant sets for the overall LTV system and the ones for each LTI model to be integrated into the tube-based robust MPC. Besides, we are also interested in the analytical methods to address the stability condition of the LTV-MPC problem with multi-model representation, apart from the LMI based numerical approach.

REFERENCES

Borrelli, F., Bemporad, A., and Morari, M. (2017). *Predictive Control for Linear and Hybrid Systems*. Cambridge University Press.

Dixon, J. (1996). *Tires, suspension and handling*. SAE.

Falcone, P., Borrelli, F., Asgari, J., Tseng, H.E., and Hrovat, D. (2007). Predictive active steering control for autonomous vehicle systems. *IEEE Transactions on Control Systems Technology*, 15(3), 566–580.

Falcone, P., Borrelli, F., Tseng, H.E., Asgari, J., and Hrovat, D. (2008). Linear time-varying model predictive control and its application to active steering systems: Stability analysis and experimental validation. *International Journal of Robust and Nonlinear Control*, 18(8), 862–875.

Gao, Y., Gray, A., Frasch, J.V., Lin, T., Tseng, E., Hedrick, J.K., and Borrelli, F. (2012). Spatial predictive control for agile semi-autonomous ground vehicles. In *Proc. of International Symposium on Advanced Vehicle Control*, 2, 1–6.

Herceg, M., Kvasnica, M., Jones, C., and Morari, M. (2013). Multi-Parametric Toolbox 3.0. In *Proc. of the European Control Conference*, 502–510. Zürich, Switzerland. `http://control.ee.ethz.ch/ mpt`.

Knight, W. (2018). What Uber's fatal accident could mean for the autonomous-car industry. *MIT Technology Review*.

Kothare, M.V., Balakrishnan, V., and Morari, M. (1996). Robust constrained model predictive control using linear matrix inequalities. *Automatica*, 32(10), 1361–1379.

Lima, P.F., Mårtensson, J., and Wahlberg, B. (2017a). Stability conditions for linear time-varying model predictive control in autonomous driving. In *Proc. of IEEE International Conference on Decision and Control (CDC)*, 2775–2782. IEEE.

Lima, P.F., Nilsson, M., Trincavelli, M., Mårtensson, J., and Wahlberg, B. (2017b). Spatial model predictive control for smooth and accurate steering of an autonomous truck. *IEEE Transactions on Intelligent Vehicles*, 2(4), 238–250.

Lima, P.F., Pereira, G.C., Mårtensson, J., and Wahlberg, B. (2018a). Experimental validation of model predictive control stability for autonomous driving. *Control Engineering Practice*, 81, 244–255.

Lima, P.F., Pereira, G.C., Mårtensson, J., and Wahlberg, B. (2018b). Progress maximization model predictive controller. In *2018 21st International Conference on Intelligent Transportation Systems (ITSC)*, 1075–1082. IEEE.

Llorca, D.F., Milanés, V., Alonso, I.P., Gavilán, M., Daza, I.G., Pérez, J., and Sotelo, M.Á. (2011). Autonomous pedestrian collision avoidance using a fuzzy steering controller. *IEEE Transactions on Intelligent Transportation Systems*, 12(2), 390–401.

Mayne, D.Q., Rawlings, J.B., Rao, C.V., and Scokaert, P.O. (2000). Constrained model predictive control: Stability and optimality. *Automatica*, 36(6), 789–814.

Shiller, Z. and Sundar, S. (1998). Emergency lane-change maneuvers of autonomous vehicles. *Journal of Dynamic Systems, Measurement, and Control*, 120(1), 37–44.

Simon, D., Löfberg, J., and Glad, T. (2012). Reference tracking mpc using terminal set scaling. In *Proc. of IEEE International Conference on Decision and Control (CDC)*, 4543–4548. IEEE.

Swaroop, D. and Yoon, S.M. (1999). Integrated lateral and longitudinal vehicle control for an emergency lane change manoeuvre design. *International Journal of Vehicle Design*, 21(2-3), 161–174.

Vanholme, B., Gruyer, D., Lusetti, B., Glaser, S., and Mammar, S. (2013). Highly automated driving on highways based on legal safety. *IEEE Transactions on Intelligent Transportation Systems*, 14(1), 333–347.